



Measurement of the $^{232}\text{Th}(n, \gamma)^{233}\text{Th}$ and $^{232}\text{Th}(n, 2n)^{231}\text{Th}$ reaction cross-sections at neutron energies of 8.04 ± 0.30 and 11.90 ± 0.35 MeV

Rita Crasta ^a, H. Naik ^{b,*}, S.V. Suryanarayana ^c, B.S. Shivashankar ^d, V.K. Mulik ^e, P.M. Prajapati ^f, Ganesh Sanjeev ^a, S.C. Sharma ^c, P.V. Bhagwat ^c, A.K. Mohanty ^c, S. Ganesan ^g, A. Goswami ^b

^a Department of Studies in Physics, Microtron Centre, Mangalore University, Mangalagangothri 574 199, Karnataka, India

^b Radiochemistry Division, Bhabha Atomic Research Centre, Mumbai 400 085, India

^c Nuclear Physics Division, Bhabha Atomic Research Centre, Mumbai 400 085, India

^d Department of statistics, Manipal University, Manipal 576 104, Karnataka, India

^e Department of Physics, University of Pune, Pune 411 007, India

^f Physics Department, The M.S. University of Baroda, Vadodara 390 002, India

^g Reactor Physics Design Division, Bhabha Atomic Research Centre, Mumbai 400 085, India

ARTICLE INFO

Article history:

Received 17 December 2011

Received in revised form 4 February 2012

Accepted 11 February 2012

Available online 1 June 2012

Keywords:

Neutron capture cross-section

Neutron activation

Off-line γ -ray spectrometric technique

$^7\text{Li}(p, n)^7\text{Be}$ reaction

Neutron energies of 8.04 ± 0.3 MeV and

11.9 ± 0.35 MeV

Talys 1.2 computer code

ABSTRACT

The $^{232}\text{Th}(n, \gamma)^{233}\text{Th}$ and $^{232}\text{Th}(n, 2n)^{231}\text{Th}$ reaction cross-sections have been determined for the first time at average neutron energies of 8.04 ± 0.30 MeV and 11.90 ± 0.35 MeV using activation and off-line γ -ray spectrometric technique. The neutron beam was generated using $^7\text{Li}(p, n)$ reaction. The experimentally determined cross-sections were compared with the evaluated nuclear data libraries of ENDF/B-VII and JENDL 4.0 and are found to be in good agreement. The $^{232}\text{Th}(n, \gamma)^{233}\text{Th}$ and $^{232}\text{Th}(n, 2n)^{231}\text{Th}$ reaction cross-sections were also calculated theoretically using TALYS 1.2 computer code and compared with the experimental data.

© 2012 Elsevier Ltd. All rights reserved.

1. Introduction

The measurement of the neutron induced reaction cross-sections such as (n, γ) , $(n, 2n)$, (n, p) and (n, α) as a function of the incident neutron energy for actinides and structural materials are of particular importance. These reaction cross-section data are required for several applications in the areas of reactor technology, applied nuclear physics, nuclear models, elemental analysis, etc. In addition to these novel options, the reaction cross-sections are useful in accelerator driven sub-critical systems (ADSs), which is considered as a promising and challenging task for transmutation of long-lived radioactive waste and power production (Rubbia et al., 1995; Carminati et al., 1993; IAEA, 1997; Bowman, 1998; Ganesan, 2007; Westmeier et al., 2005). The thorium based nuclear fuel cycle offers many advantages. The

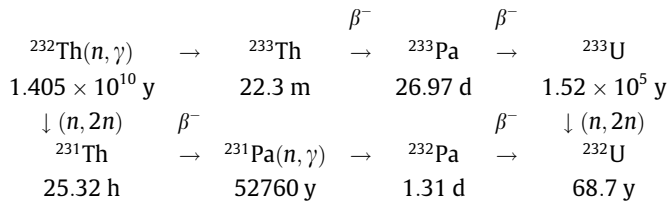
* Corresponding author. Tel.: +91 22 25594574; fax: +91 22 25505151 (O), 25519613.

E-mail address: naikhbarc@yahoo.com (H. Naik).

^{232}Th – ^{233}U fuel cycle is studied extensively for power production and as a waste management option in the next generation of systems like ADSs (Rubbia et al., 1995; Carminati et al., 1993; IAEA, 1997; Bowman, 1998; Ganesan, 2007; Westmeier et al., 2005), AHWR (Sinha and Kakodkar, 2006) and fast reactors (Mathieu et al., 2005; IAEA, 2002; Nuttin et al., 2005). Thorium fuel is an attractive way to produce long term nuclear energy with low radio toxicity waste.

The abundance of thorium in the earth crust is three to four times that of uranium, thus the thorium fuel cycle ensures a long term supply of nuclear fuel. Because of its relatively high natural abundance, ^{232}Th is gaining importance as a fertile isotope for future nuclear reactors. The thorium–uranium fuel cycle is based on the fertile ^{232}Th and the fissile ^{233}U , formed by neutron capture on ^{232}Th and the subsequent β -decays of ^{233}Th and ^{233}Pa . The neutron capture reaction cross-section of ^{232}Th is an important parameter for the design of any nuclear reactor based on the ^{232}Th – ^{233}U fuel cycle.

The nuclide ^{233}U and ^{232}U is formed by the $^{232}\text{Th}(n, \gamma)^{233}\text{Th}$ and $^{232}\text{Th}(n, 2n)^{231}\text{Th}$ reaction according to the scheme



The production of the fissile nucleus ^{233}U depends on the $^{232}\text{Th}(n, \gamma)$ reaction cross-section, which is required with an accuracy of 1–2% to be used safely in simulation techniques for prediction, the dynamical behavior of complex arrangements in fast reactors or ADSs (Pronyayev, 1999; Kuzminov and Manokhin, 1997). The importance of $^{232}\text{Th}(n, \gamma)$ reaction cross-section at higher neutron energy has a strong impact on the performance and safety assessment for ADSs. A 10% uncertainty in the reaction cross-section of $^{232}\text{Th}(n, \gamma)$ can produce 30% uncertainty in the proton current requirement to operate an ADSs at the sub-critical level of $k_{\text{eff}} \approx 0.97$ (Salvatores, 1997).

There are some measurements of $^{232}\text{Th}(n, \gamma)$ reaction cross-section from thermal to 2.73 MeV in the last few years using activation technique (Pomerance, 1952; Macklin et al., 1957; Stupegia et al., 1963; Forman et al., 1971; Lindner et al., 1976; Baldwin and Knoll, 1984; Jones et al., 1986; Wisshak et al., 2001; Karamanis et al., 2001). However, only three experimental data are available for the neutron energy beyond 2.73 MeV using activation techniques, one at 14.8 MeV by Perkin et al., 1958, two at 3.70 ± 0.30 and 9.85 ± 0.38 MeV by Naik et al., 2011. At the neutron energy higher than 6.44 MeV, $^{232}\text{Th}(n, 2n)$ reaction starts and becomes the predominant mode besides fission and inelastic reaction channels. Sufficient data on the $^{232}\text{Th}(n, 2n)$ reaction cross-section at different neutron energies are available in literature (Butler and Santry, 1961; Bormann, 1965; Chatani, 1983; Raics et al., 1985; Karamanis et al., 2003; Adam et al., 2005). Adjacent to the neutron energy of 6.44 MeV there is no $^{232}\text{Th}(n, \gamma)$ reaction cross-section data available to examine its trend, where the $^{232}\text{Th}(n, 2n)$ reaction starts. In the present work, the neutron capture cross-section of ^{232}Th was measured at the average neutron energy of 8.04 ± 0.30 MeV and 11.90 ± 0.35 MeV. The neutron beam was produced by using $^7\text{Li}(p, n)$ reaction. The activation method followed by off-line γ -ray spectrometric technique was used for the present work. Using the same technique, $^{232}\text{Th}(n, 2n)$ reaction cross-section is also determined at average neutron energy of 8.04 ± 0.30 MeV and 11.90 ± 0.35 MeV. The experimentally obtained reaction cross-sections were compared with the evaluated nuclear data libraries of ENDF/B-VII.0 (Chadwick et al., 2006), JENDL 4.0 (Shibata et al., 2011), and JEFF-3.1 (Koning et al., 2007). Theoretically, the present experimental data have been analyzed on the basis of the TALYS 1.2 reaction code (Koning et al., 2005).

2. Description of the experiment

Average neutron energy of 8.04 ± 0.30 and 11.90 ± 0.35 MeV were produced by the $^7\text{Li}(p, n)$ reaction at proton energy of 10 and 14 MeV, using the 14 UD BARC-TIFR Pelletron facility at Mumbai, India. The lithium foil was made up of natural lithium with thickness 3.7 mg/cm^2 and is sandwiched between two tantalum foils of different thicknesses. The thinner tantalum foil facing the proton beam with thickness of 4 mg/cm^2 , in which the degradation of the proton energy is only 30 keV. The thicker tantalum foil of 0.025 mm, which is located behind the lithium foil, is sufficient to stop the proton beam. Behind the Ta–Li–Ta stack, the natural thorium metal foil with thickness 143.8 mg/cm^2 was placed for irradiation. The Th foil was wrapped with 0.025 mm thick super

pure aluminum foil and mounted at zero degree with respect to the beam direction at a distance of 2.0 cm from the location of the Ta–Li–Ta stack. The experimental arrangement is shown in Fig. 1. The isotopic abundance of ^{232}Th in natural thorium is 100%.

Different sets were made for different irradiations at various neutron energies. Both the samples were irradiated for 5–7 h depending upon the proton beam energy facing the tantalum target. The proton beam energies were 10 and 14 MeV and the proton current during the irradiation was 270 nA at 10 MeV and 300 nA at 14 MeV. The maximum neutron energies facing the Th sample targets were 8.04 ± 0.30 MeV and 11.90 ± 0.35 MeV respectively. The activity measurements of the irradiated samples were started after sufficient cooling time. Then, the irradiated samples along with the aluminum wrapper were mounted on Perspex plates and taken for γ -ray spectrometry. The activities of the radio nuclides produced from irradiated Th samples were measured using energy- and efficiency-calibrated 80 cm^3 HPGe detector coupled to PC-based 4 K channel analyzer. The measurements were repeated for several times to follow the decay of the radio nuclides. Measurements were done at suitable distance between the sample and the end cap of the detector to keep the dead time within 5%. The detection efficiency as a function of the photon energy was determined by using the standard ^{152}Eu source. A typical γ -ray spectrum from the irradiated ^{232}Th sample for $^{232}\text{Th}(n, \gamma)$ and $^{232}\text{Th}(n, 2n)$ reactions are given in Figs. 2 and 3 respectively.

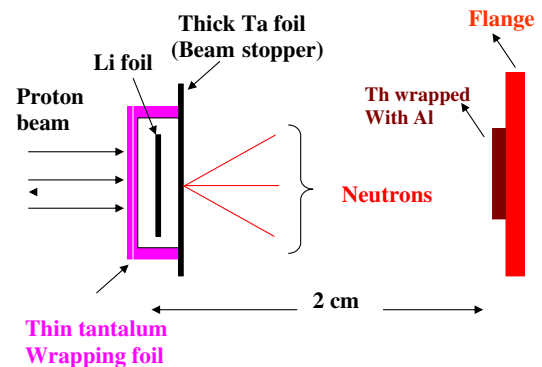


Fig. 1. Schematic diagram showing the arrangement used for neutron irradiation.

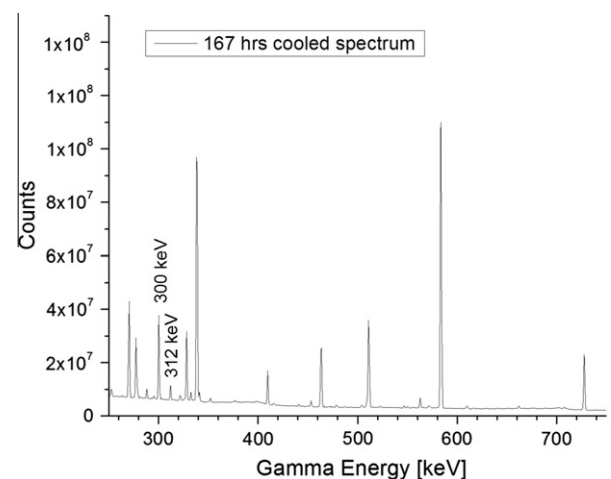


Fig. 2. Typical γ -ray spectrum of irradiated natural Th metal shows the γ -ray energies for $^{232}\text{Th}(n, \gamma)$ reaction.

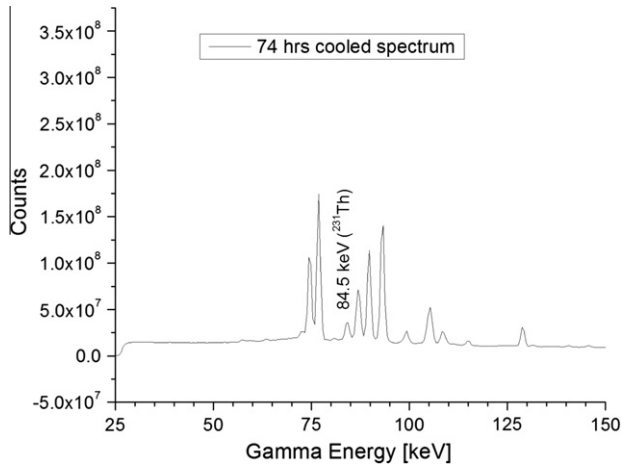


Fig. 3. Typical γ -ray energy of irradiated natural Th metal shows the γ -ray energy for $^{232}\text{Th}(n,2n)$ reaction.

3. Analysis of the experiment and results

3.1. Calculation of the neutron energy

Natural lithium consists of isotopes ^6Li and ^7Li with abundances 7.42% and 92.58% respectively. Neutrons are generated by the $^7\text{Li}(p,n)$ reaction. The Q-value for the $^7\text{Li}(p,n)^7\text{Be}$ reaction to the ground state is -1.644 MeV, whereas for the first excited state is 0.431 MeV above the ground state leading to an average Q-value of -2.079 MeV. The selected proton energies for the experiment are 10 and 14 MeV. The degradation of the proton energy on the front thin tantalum foil of 4 mg/cm^2 thickness is only 30 keV. The ground state of ^7Be is having the threshold of 1.881 MeV whereas the first excited state of ^7Be is having the threshold of 2.38 MeV. With ^7Li , a second neutron group at $E_p \geq 2.4$ MeV is produced due to the population of the first excited state of ^7Be . Thus for the proton energy of 10 and 14 MeV, the corresponding first group of (n_0) neutron energies are 8.12 and 12.12 MeV to the ground state of ^7Be . For the first excited state of ^7Be , the neutron energy of the second group of neutrons (n_1) will be 7.62 and 11.62 MeV respectively. Fragmentation of ^8Be to $^4\text{He} + ^3\text{He} + n$ ($Q = -3.23$ MeV) also occurs when the proton energy exceeds the value 4.5 MeV and the other reaction channels are open to give continuous neutron distribution besides n_0 and n_1 groups of neutrons. The branching ratio to the ground and first excited state of ^7Be up to proton energy of 7 MeV is given in Refs. Liskien and Paulsen (1975) and Meadows and Smith (1972), whereas for proton energies from 4.2 MeV to 26 MeV is given in Ref. Poppe et al. (1976). The neutron spectrum has continuous tailing besides n_0 and n_1 group of neutrons, for the proton energies of 10 and 14 MeV. The neutron spectra for these proton energies were generated as done by Naik et al., 2011, using the neutron energy distribution given in Refs. Poppe et al. (1976) and Mashnik et al. (2008). The generated neutron spectra of the present work at proton energy of 10 and 14 MeV are similar to the distribution shown by Naik et al., 2011 for proton energy of 12 MeV. For the proton energy of 10 MeV, the tailing part of the distribution of the neutron spectrum below 6 MeV has been removed to obtain the average neutron energy under the main peak region, which is 8.04 ± 0.30 MeV. The uncertainty of the neutron energy arises due to the spread of the neutron distribution (width) consisting of n_0 and n_1 group of neutrons. Similarly for the proton energy of 14 MeV, the average neutron energies under the main peak region was obtained as 11.90 ± 0.35 MeV after removing the tailing distribution of the neutron spectrum below 10.5 MeV.

3.2. Calculation of the neutron flux

The neutron flux is usually obtained by using $^{197}\text{Au}(n,\gamma)^{198}\text{Au}$ and $^{115}\text{In}(n,n^1)^{115\text{m}}\text{In}$ reaction cross-sections for mono-energetic nuclear reactions. For thermal neutrons the photo peak activity of the 411.8 keV γ -line for ^{198}Au from $^{197}\text{Au}(n,\gamma)$ reaction is used to find the neutron flux. For higher energy neutrons the photo peak activity of the 336.2 keV γ -line of the $^{115\text{m}}\text{In}$ from the $^{115}\text{In}(n,n^1)$ reaction is used for flux determination. In the present work the neutron beam was produced from $^7\text{Li}(p,n)$ reaction, where the neutron energy is on higher side and not exactly mono-energetic. This is due to the contribution from the second group as well as a tailing resulting from the break up $^8\text{Be} \rightarrow ^4\text{He} + ^3\text{He} + n$, which has a significant contribution. It can be seen from Refs. Poppe et al. (1976) and Mashnik et al. (2008) that tailing region of the low energy neutrons is quite significant. Within this range of neutron energy, the $^{115}\text{In}(n,n^1)^{115\text{m}}\text{In}$ reaction cross-sections changes continuously (The International Reactor Dosimetry file, 2002). On the other hand, the neutron-induced fission cross-section of ^{232}Th (Blons et al., 1975) has a step function, whereas the yields of fission products (Glendenin et al., 1980) at peak position of the mass-yield curve do not change significantly. For this purpose, the neutron flux was calculated using the yield (Y) of fission products as ^{135}I and ^{97}Zr , extracted from the experimental yields of Ref. Glendenin et al. (1980) and Crouch (1977) in the neutron induced fission of ^{232}Th . The neutron flux and the observed photo peak activities (A_{obs}) for γ -lines of the respective nuclide are related by the equation,

$$\phi = \frac{A_{\text{obs}}(\text{CL/LT})\lambda}{N\sigma_f Y a \varepsilon (1 - e^{-\lambda t})(e^{-\lambda T})(1 - e^{-\lambda \text{CL}})} \quad (1)$$

where N is the number of target atoms. σ_f is the fission cross-section taken from Refs. Henkel (1957) and Paradelo et al. (2006), Y is the yield of the fission product taken from Ref. Glendenin et al. (1980) and Crouch (1977), ' a ' is the branching intensity and ε is detection efficiency for γ -lines of the nuclide of interest. ' t ' and T are the irradiation and cooling times whereas, CL and LT are the clock time and live time of counting, respectively. In the above equation the CL/LT term has been used for dead time correction. The γ -ray energies and the nuclear spectroscopic data such as the half-lives and branching ratios of the reaction products are taken from Refs. Blachot (2005), Singh and Tuli (2005) and Browne (2001) and given in Table 1.

The neutron flux calculated using Eq. (1) for 8.04 ± 0.30 MeV and 11.90 ± 0.35 MeV neutron energies are obtained to be $(3.56 \pm 0.03) \times 10^6$ and $(1.30 \pm 0.02) \times 10^7$ $\text{n cm}^{-2} \text{s}^{-1}$ corresponding to the proton energy of 10 and 14 MeV, respectively. The neutron flux for the $^{232}\text{Th}(n,2n)$ reaction at the average neutron energies of 8.04 ± 0.30 MeV and 11.90 ± 0.35 MeV were obtained as $(2.34 \pm 0.02) \times 10^6$ and $(9.06 \pm 0.02) \times 10^6$ $\text{n cm}^{-2} \text{s}^{-1}$, respectively. These values were obtained based on the ratio of neutron flux of the neutron spectrum of Refs. Poppe et al. (1976) and Mashnik et al. (2008) for ($n,2n$) reaction above its threshold to total flux.

3.3. Determination of $^{232}\text{Th}(n,\gamma)^{233}\text{Th}$ and $^{232}\text{Th}(n,2n)^{231}\text{Th}$ reaction cross-sections and their results

The neutron irradiation on ^{232}Th target resulted in the production of ^{233}Th radio-nuclide through (n,γ) reaction process and ^{231}Th radio nuclide through ($n,2n$) process. The decay data of the radio-active products contributing reaction process and threshold energy are taken from Refs. Singh and Tuli (2005), Browne (2001) and Browne and Firestone (1986) are presented in Table 1. The unstable radio-nuclide ^{233}Th ($t_{1/2} = 21.83$ m), which is produced by the $^{232}\text{Th}(n,\gamma)^{233}\text{Th}$ nuclear reaction decays to ^{233}Pa

Table 1
Nuclear spectroscopic data used in the calculation.

Nuclide	Half life	γ -Ray energy (keV)	γ -Ray abundance (%)	References
^{231}Th	25.52 h	84.2	6.6	(Singh and Tuli)
^{233}Th	21.83 m	86.5	2.7	(Browne)
^{233}Pa	26.975 d	311.9	38.4	(Browne)

Table 2
 $^{232}\text{Th}(n, \gamma)$ and $(n, 2n)$ reaction cross-sections at different neutron energies.

Neutron energy (MeV)	Neutron flux ($\text{n cm}^{-2} \text{s}^{-1}$)	Cross section (mb)		
		Experimental	ENDF/B-VII.0	JENDL-4.0
$^{232}\text{Th}(n, \gamma)$				
8.04 \pm 0.30	$(3.56 \pm 0.03) \times 10^6$	0.77 \pm 0.08	0.703–0.816 ^a	0.93–1.068 ^b
11.90 \pm 0.35	$(1.30 \pm 0.02) \times 10^7$	1.12 \pm 0.02	1.182–1.157 ^c	1.497–1.398 ^d
$^{232}\text{Th}(n, 2n)$				
8.04 \pm 0.30	$(2.34 \pm 0.02) \times 10^6$	1566.29 \pm 62.11	1146.33–1734.4 ^a	1304.87–1904.0 ^b
11.90 \pm 0.35	$(9.06 \pm 0.02) \times 10^6$	2097.93 \pm 25.13	2181.9–2165.44 ^c	2265.98–2270.1 ^d

^a For $^{232}\text{Th}(n, \gamma)$ and $(n, 2n)$ reaction the neutron energy ranges are 7.5–8.5 MeV.

^b For $^{232}\text{Th}(n, \gamma)$ and $(n, 2n)$ reaction the neutron energy ranges are 7.5–9.0 MeV.

^c For $^{232}\text{Th}(n, \gamma)$ and $(n, 2n)$ reaction the neutron energy ranges are 11.0–12.6 MeV.

^d For $^{232}\text{Th}(n, \gamma)$ and $(n, 2n)$ reaction the neutron energy ranges are 11.0–12.5 MeV.

($t_{1/2} = 26.975$ d) by β^- decay process. In view of this, the $^{232}\text{Th}(n, \gamma)$ reaction cross-section was calculated from the observed photo-peak activity of ^{233}Pa from the γ -ray spectrum of the long cooled sample. So the ^{233}Pa radio-nuclide was identified through an analysis of the 311.9 keV characteristic γ -line. Similarly, the $^{232}\text{Th}(n, 2n)$ reaction cross-section was calculated from the observed photo-peak activity of the 84.2 keV γ -line of ^{231}Th from the γ -ray spectrum of a sufficiently cooled sample.

The number of detected γ -rays (A_{obs}) of the reaction products ^{233}Th and ^{231}Th was used to calculate the neutron induced reaction cross-section of ^{232}Th using Eq. (1) and is rewritten as

$$\sigma = \frac{A_{\text{obs}} \left(\frac{\text{CL}}{\text{LT}} \right) \lambda}{N \phi a \varepsilon (1 - e^{-\lambda t}) (e^{-\lambda T}) (1 - e^{-\lambda \text{CL}})} \quad (2)$$

All terms in Eq. (2) have the same meaning as in Eq. (1). At an average neutron energy of 8.04 \pm 0.30 MeV, the $^{232}\text{Th}(n, \gamma)$ reaction cross-section obtained to be 4.52 \pm 0.08 mb for neutron flux of $(3.56 \pm 0.03) \times 10^6 \text{ n cm}^{-2} \text{ s}^{-1}$. Similarly, for average neutron energy of 11.90 \pm 0.35 MeV, for the same reaction the cross-section obtained to be 2.24 \pm 0.02 mb for the neutron flux of $(1.30 \pm 0.02) \times 10^7 \text{ n cm}^{-2} \text{ s}^{-1}$. At an average neutron energy of 8.04 \pm 0.30 MeV, the neutron flux of $(2.34 \pm 0.02) \times 10^6 \text{ n cm}^{-2} \text{ s}^{-1}$ was used to calculate the $^{232}\text{Th}(n, 2n)$ reaction cross-section, which is 1566.29 \pm 62.11 mb. Similarly at an average neutron energy of 11.9 \pm 0.35 MeV, the neutron flux of $(9.06 \pm 0.02) \times 10^6 \text{ n cm}^{-2} \text{ s}^{-1}$ was used to calculate the $^{232}\text{Th}(n, 2n)$ reaction cross-section, which is 2097.93 \pm 25.13 mb. At same neutron energy, lower neutron flux used for the $^{232}\text{Th}(n, 2n)$ reaction cross-section calculation compared to $^{232}\text{Th}(n, \gamma)$ reaction is based on the threshold value of 6.44 MeV for the former reaction.

The $^{232}\text{Th}(n, \gamma)$ cross-section values of 4.52 \pm 0.08 mb at neutron energy of 8.04 \pm 0.30 MeV and 2.24 \pm 0.02 mb at 11.90 \pm 0.35 MeV are slightly higher because of the contribution from the low energy neutron reaction cross-section. This contribution of the cross-section from the tail region to the $^{232}\text{Th}(n, \gamma)$ reaction has been estimated using the ENDF/B-VII.0 (Chadwick et al., 2006) and JENDL-4.0 (Shibata et al., 2011) by folding the cross-sections with neutron flux distributions of Refs. Poppe et al. (1976) and Mashnik et al. (2008). At proton energy of 10 MeV, the contribution of the cross-sections to the $^{232}\text{Th}(n, \gamma)$ reaction was evaluated to be 3.55

and 3.95 mb from ENDF/B-VII.0 (Chadwick et al., 2006), JENDL-4.0 (Shibata et al., 2011), respectively. Similarly, contribution to the $^{232}\text{Th}(n, \gamma)$ reaction from the above evaluations at proton energy of 14 MeV are 1.02 mb and 1.22 mb from ENDF/B-VII.0 (Chadwick et al., 2006), JENDL-4.0 (Shibata et al., 2011) respectively.

The actual experimentally obtained cross-section for $^{232}\text{Th}(n, \gamma)$ reaction, after removing the contribution from the tail region was obtained to be 0.77 \pm 0.08 mb and 1.12 \pm 0.02 mb at an average neutron energies of 8.04 \pm 0.30 and 11.90 \pm 0.35 MeV, corresponding to the proton energies of 10 MeV and 14 MeV, which are given in Table 2. At an average neutron energies of 8.04 \pm 0.30 and 11.90 \pm 0.35 MeV, corresponding to the proton energies of 10 and 14 MeV, the $^{232}\text{Th}(n, 2n)^{231}\text{Th}$ reaction cross-section were obtained to be 1566.29 \pm 62.11 mb and 2097.93 \pm 25.13 mb, which are also given in Table 2.

The uncertainties associated to the measured cross-sections come from the combination of two experimental data sets. This overall uncertainty is the quadratic sum of both statistical and systematic errors. The random error in the observed activity is primarily due to counting statistics, which is estimated to be 5–10%. This can be determined by accumulating the data for an optimum time period that depends on the half-life of nuclides of interest. The systematic errors are due to uncertainties in photon flux estimation (\sim 2%), the irradiation time (\sim 0.5%), the detection efficiency calibration (\sim 3%), the half-life of the reaction products and the γ -ray abundances (\sim 2%) as reported in the literature (Blachot, 2005; Singh and Tuli, 2005; Browne, 2001). Thus the total systematic error is about \sim 4.2%. The overall uncertainty is found to range between 6.5% and 10.8%, coming from the combination of a statistical error of 5–10% and a systematic error of 4.2%.

4. Discussions

The neutron induced reaction cross-section of the $^{232}\text{Th}(n, \gamma)$ reaction measured in the present work at average neutron energies of 8.04 \pm 0.30 and 11.90 \pm 0.35 MeV (Table 2) are determined for the first time. On the other hand the $^{232}\text{Th}(n, 2n)$ reaction cross-section from the present work at average neutron energy of 8.04 \pm 0.30 MeV and 11.90 \pm 0.35 MeV (Table 2) are the re-determined value. The experimentally obtained reaction cross-section

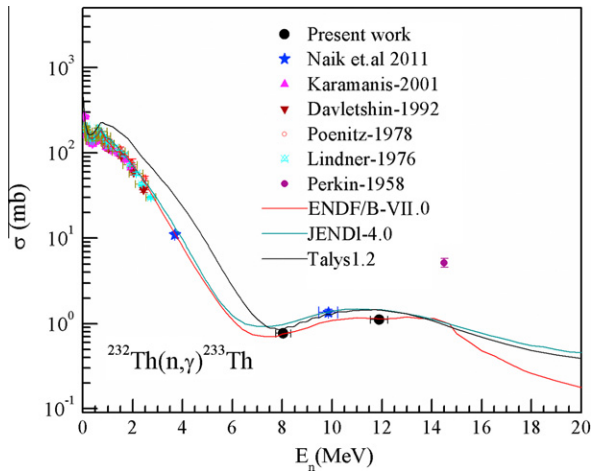


Fig. 4. Plot of experimental, theoretical and evaluated $^{232}\text{Th}(n,\gamma)$ reaction cross-section as a function of neutron energy.

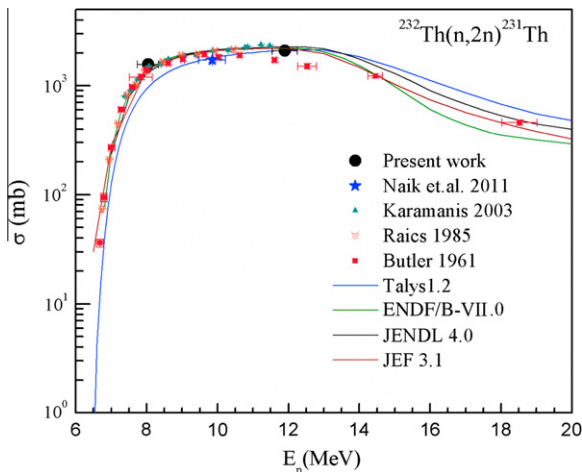


Fig. 5. Plot of experimental, theoretical and evaluated $^{232}\text{Th}(n,2n)$ reaction cross-section as a function of neutron energy.

for the $^{232}\text{Th}(n,\gamma)$ and $^{232}\text{Th}(n,2n)$ nuclear reactions were compared with the evaluated data from ENDF/B-VII.0 (Chadwick et al., 2006) and JENDL-4.0 (Shibata et al., 2011) are quoted in Table 2. These evaluated reaction cross-sections given in Table 2 within the neutron energy range from 7.5 to 8.5 MeV and 11 to 12.5 MeV for $^{232}\text{Th}(n,\gamma)$ and $^{232}\text{Th}(n,2n)$ reactions is due to the finite width of the neutron energy under the main peak (Poppe et al., 1976; Mashnik et al., 2008).

The experimentally obtained $^{232}\text{Th}(n,\gamma)$ and $^{232}\text{Th}(n,2n)$ reaction cross-sections at average neutron energies of 8.04 ± 0.30 and 11.90 ± 0.35 MeV are within the range of evaluated data (Table 2). In order to examine this aspect, the $^{232}\text{Th}(n,\gamma)$ reaction cross-section from present work along with literature data (Naik et al., 2011; Lindner et al., 1976; Karamanis et al., 2001; Perkin et al., 1958; Davletshin et al., 1992; Poenitz and Smith, 1978), given in EXFOR (IAEA, EXFOR) as well as evaluated data from ENDF/B-VII.0, JENDL-4.0 were plotted in Fig. 4. It can be seen from Fig. 4 that the evaluated $^{232}\text{Th}(n,\gamma)$ reaction cross-section decreases up to a neutron energy of 8 MeV and thereafter increases. Higher value of the $^{232}\text{Th}(n,\gamma)$ reaction cross-section at neutron energy above 8 MeV may be due to the saturation of neutron emission (n,2n) and (n,nf) cross-sections. Theoretically, the $^{232}\text{Th}(n,\gamma)$ and $^{232}\text{Th}(n,2n)$ reaction cross-sections at neutron

energy beyond 1 keV were also calculated using computer code TALYS version 1.2 (Koning et al., 2005). TALYS is a computer code basically used for analysis of basic scientific experiments or to generate nuclear data for applications. The basic objective behind its construction is the simulation of nuclear reactions that involve neutrons, photons, protons, deuterons, tritons, ^3He - and alpha-particles, in the 1 keV to 200 MeV energy range and for target nuclides of mass 12 and heavier. In TALYS, cross-section for reactions to all open channels is calculated. Several options are included for the choice of different parameters such as γ -strength functions, nuclear level densities and nuclear model parameters etc. All possible outgoing channels possible for the given neutron energy were considered. However, the cross-section for the (n, γ) and (n,2n) reaction was specially looked for and collected. Theoretically obtained $^{232}\text{Th}(n,\gamma)$ and $^{232}\text{Th}(n,2n)$ reaction cross-section using TALYS 1.2 computer code are also plotted in Figs. 4 and 5.

It can be seen from Fig. 4 that, the trend of the experimental and evaluated $^{232}\text{Th}(n,\gamma)$ reaction cross-section is well reproduced by the TALYS 1.2 computer code. However, the $^{232}\text{Th}(n,\gamma)$ reaction cross-section calculated from TALYS are slightly higher than the experimental and evaluated data for neutron energy from 100 keV to 9.85 MeV but lower than the values at neutron energy of 14.5 MeV. This is because in the TALYS the fission cross-section as a function of the neutron energy is quantitatively not well accounted, though the trend is reproduced. Similar to the evaluated data, the $^{232}\text{Th}(n,\gamma)$ reaction cross-section calculated theoretically using TALYS 1.2 code shows a dip at a neutron energy of 7.3–8.5 MeV. The dip in the $^{232}\text{Th}(n,\gamma)$ reaction cross-section around a neutron energy of 7.5–8.5 MeV indicates the opening of the (n,2n) reaction channel besides the (n,nf) channel. To verify this, $^{232}\text{Th}(n,2n)$ reaction cross-sections from the present work and from the literature (Naik et al., 2011; Butler and Santry, 1961; Raics et al., 1985; Karamanis et al., 2003) along with the theoretical (Koning et al., 2005) and evaluated data (Chadwick et al., 2006; Shibata et al., 2011; Koning et al., 2007) were plotted in Fig. 5.

It can be seen from Fig. 5 that the experimental and theoretical $^{232}\text{Th}(n,2n)$ reaction cross-section shows a sharp increasing trend from the neutron energy of 6.6 MeV to 8.0 MeV and thereafter remains constant up to 14.5 MeV. Thus, the increasing trend of $^{232}\text{Th}(n,\gamma)$ reaction cross section beyond 8 MeV up to 14.5 MeV (Fig. 4) is due to constant $^{232}\text{Th}(n,2n)$ reaction cross-section (Fig. 5). Furthermore, it can be seen from Figs. 4 and 5 that the $^{232}\text{Th}(n,\gamma)$ reaction cross-section shows a dip, where the $^{232}\text{Th}(n,2n)$ reaction cross-section shows a sharp increasing trend. This is most probably due to the sharing of the excitation energy between $^{232}\text{Th}(n,\gamma)$ and (n,2n) reaction channels in the neutron energy range below 14 MeV. Above the neutron energy of 14 MeV, $^{232}\text{Th}(n,\gamma)$ and (n,2n) reaction cross-sections show a decreasing trend due to opening of (n,3n) reaction channels.

5. Conclusions

- The $^{232}\text{Th}(n,\gamma)^{233}\text{Th}$ reaction cross-sections at an average neutron energies of 8.04 ± 0.30 and 11.90 ± 0.35 MeV have been determined for the first time. On the other hand, the $^{232}\text{Th}(n,2n)^{231}\text{Th}$ reaction cross-section at neutron energy of 8.04 ± 0.30 MeV and 11.90 ± 0.35 MeV are the re-determined values, which are in agreement with the literature data.
- The $^{232}\text{Th}(n,\gamma)$ and $^{232}\text{Th}(n,2n)$ reaction cross-sections at average neutron energies of 8.04 ± 0.30 and 11.90 ± 0.35 MeV are in good agreement with the evaluated data from ENDF/B-VII.0, JENDL-4.0 and JEFF 3.1.

(c) The $^{232}\text{Th}(n, \gamma)$ and $^{232}\text{Th}(n, 2n)$ reaction cross-sections were also calculated using the TALYS 1.2 computer code and found to be in general agreement with the experimentally measured data.

Acknowledgements

The authors are thankful to the staff of TIFR-BARC Pelletron facility for their kind co-operation and help to provide the proton beam to carry out the experiment. We are also thankful to Mr. Ajit Mahadakar and Mrs. Deepa Thapa from target laboratory of Pelletron facility at TIFR, Mumbai for providing us the Li and Ta targets. Financial support from the Research in Nuclear sciences (BRNS), DAE, Government of India, is gratefully acknowledged by one of the authors Mrs. Rita Crasta. The authors wish to thank fellow researchers and technical staffs at the Microtron Centre, Mangalore University for their help.

References

- Adam, J., Balabekyan, A.R., Barashenkov, V.S., Brandt, R., Golovatiouk, V.M., Kalinnikov, V.G., Katovsky, K., Krivopustov, Kumar, M.I.V., Kumawat, H., Odoj, R., Pronskikh, V.S., Solnyshkin, A.A., Stegailov, V.I., Tsoumpko-Sitnikov, V.M., Westmeier, W., 2005. Spallation neutron spectrum on a massive lead/paraffin target irradiated with 1 GeV protons. *Eur. Phys. J. A* 23, 61–68.
- Baldwin, G.T., Knoll, G.F., 1984. Absolute measurement of the cross-section for 23 keV neutron activation of thorium. *Nucl. Sci. Eng.* 88, 123–128.
- Blachot, J., 2005. Nuclear data sheets for A = 115*. *Nucl. Data Sheets* 104, 967–1110.
- Blons, J., Mazur, C., Paya, D., 1975. Evidence for rotational bands near the $^{232}\text{Th}(n, f)$ fission threshold. *Phys. Rev. Lett.* 35, 1749–1751.
- Bormann, M., 1965. Neutron shell effects in the (n, 2n) cross sections at 14 MeV. *Nucl. Phys.* 65, 257–274.
- Bowman, C.D., 1998. Accelerator-driven systems for nuclear waste transmutation. *Ann. Rev. Nucl. Part. Sci.* 48, 505–556.
- Browne, E., 2001. Nuclear data sheets for A = 215, 219, 223, 227, 231. *Nucl. Data Sheets* 93, 763–1061.
- Browne, E., Firestone, R.B., 1986. In: Shirley, V.S. (Ed.), *Table of Radioactive Isotopes*. John Wiley & Sons, New York.
- Butler, J.P., Santry, D.C., 1961. $^{232}\text{Th}(n, 2n)^{231}\text{Th}$ cross section from threshold to 20. *Can. J. Chem.* 39, 689–696.
- Carminati, F., Klapisch, R., Revol, J.P., Roche, Ch., Rubio, J.A., Rubbia, C., 1993. An Energy Amplifier for Cleaner and Inexhaustible Nuclear Energy Production Driven by Particle Beam Accelerator, CERN Report No. CERN/AT/93-47 (ET).
- Chadwick, M.B. et al., 2006. ENDF/B-VII.0: next generation evaluated nuclear data library for nuclear science and technology. *Nucl. Data Sheets* 107, 2931–3060.
- Chatani, H., 1983. A measurement of the averaged cross section for the $^{232}\text{Th}(n, 2n)^{231}\text{Th}$ reaction with a fission plate. *Nucl. Inst. Methods* 205, 501–504.
- Crouch, E.A.C., 1977. Fission product yields from neutron-induced fission. *Atom. Data. Nucl. Data Tables* 19, 419–532.
- Davletshin, A.N., Teplov, E.V., Tipunko, A.O., Pravdivy, N.M., Sklyar, N.T., Mishchenko, V.A., 1992. Neutron Radiative capture cross-section for ^{232}Th and ^{197}Au in the neutron energy range 0.8–2.5 MeV. *J. Vop. At.Nauki, Tekhn., Ser. Yadernye Konstanty* (1), 41–74.
- Forman, L., Schelberg, A.D., Warren, J.H., Glass, N.W., 1971. ^{232}Th neutron capture in region 20 eV–30 eV. *Phys. Rev. Lett.* 27, 117–120.
- Ganesan, S., 2007. Nuclear data requirements for accelerator driven sub-critical systems – a roadmap in the Indian context *Pramana. J. Phys.* 68, 257–268.
- Glendenin, L.E., Gindler, J.E., Ahmad, I., Henderson, D.J., Meadows, J.W., 1980. Mass distributions in monoenergetic-neutron-induced fission of ^{232}Th . *Phys. Rev. C* 22, 152–159.
- Henkel, R.L., 1957. Fast Neutron Cross Sections: Corrections to LA-1714 and a Correlation of 3 MeV values. Los Alamos Scientific Lab. Reports No. LA-2122.
- IAEA-TECDOC-1319, 2002. Fast Reactors and Accelerator Driven Systems Knowledge Base, Energy Generation and Thorium fuel utilization: Options and Trends. (November).
- IAEA-TECDOC-985, 1997. Accelerator Driven Systems: Energy Generation and Transmutation of nuclear waste, Status report. (November).
- IAEA-EXFOR, Experimental Nuclear Reaction Data. <<http://www-nds.iaea.org/exfor>>.
- Jones, R.T., Merritt, J.S., Okazaki, A., 1986. Measurement of the thermal neutron capture cross-section of ^{232}Th . *Nucl. Sci. Eng.* 93, 171–180.
- Karamanis, D., Andriamonje, S., Assimakopoulos, P.A., Dourkellis, G., Karademos, D.A., Karydas, A., Kokkoris, M., Korrsionides, S., Nicolis, N.G., Papachristodoulou, C., Papadopoulos, C.T., Patronis, N., Pavlopoulos, P., Perdikakis, G., Vlastos, R., 2003. Neutron cross section measurements in the Th–U cycle by the activation method. The n-TOF Collaboration. *Nucl. Instrum. Methods Phys. Res. A* 505, 381–384.
- Karamanis, D., Petit, M., Andriamonje, S., Barreau, G., Bercion, M., Billebaud, A., Blank, B., Czajkowski, S., Del Moral, R., Giovinazzo, J., Lacoste, V., Marchand, C., Perrot, L., Pravikoff, M., Thomas, J.C., 2001. Neutron radiative capture cross sections of ^{232}Th in the energy range from 0.06–2 MeV. *Nucl. Sci. Eng.* 139, 282–293.
- Koning, A.J., et al., 2007. The JEFF evaluated data project. In: Proc. of the International Conf. on Nuclear Data for Science and Technology, Nice, 2007 (EDP Sciences, 2008).
- Koning, A.J., Hilaire, S., Duijvestijn, M.C., 2005. In: Haight, R.C., Chadwick, M.B., Kawano, T., Talou, P., (Eds.), Proceedings of the International Conference on Nuclear Data for Science and Technology, ND 2004, Santa Fe, 2004, AIP Conf. Proc. 769, pp. 1154–1159.
- Kuzminov, B.D., Manokhin, V.N., 1997. Status of nuclear data for thorium fuel cycle. *Nucl. Constants* (3–4), 41.
- Lindner, M., Nagle, R.J., Landrum, J.H., 1976. Neutron capture cross-sections from 0.1 to 3 MeV by activation measurements. *Nucl. Sci. Eng.* 59, 381–394.
- Liskien, H., Paulsen, A., 1975. Neutron production cross sections and energies for the reactions $^7\text{Li}(p, n)^7\text{Be}$ and $^7\text{Li}(p, n)^7\text{Be}^*$. *At. Data Nucl. Data Tables* 15, 57–84.
- Macklin, R.L., Lazar, N.H., Lyon, W.S., 1957. Neutron activation cross sections with Sb–Be neutrons. *Phys. Rev.* 107, 504–508.
- Mashnik, S.G., Chadwick, M.B., Hughes, H.G., Little, R.C., Macfarlane, R.E., Waters, L.S., Young, P.G., 2008. $^7\text{Li}(p, n)$ Nuclear Data Library for Incident Proton Energies to 150 MeV. Los Alamos National Laboratory, Los Alamos, NM 87545, USA. (February 8).
- Mathieu, L., et al., 2005. Proportion for a very simple thorium molten salt reactor. In: Proceedings of the Global International Conference, Tsukuba, Japan, Paper No. 428.
- Meadows, J.W., Smith, D.L., 1972. Neutrons from proton bombardment of natural Lithium. Argon National Laboratory Report ANL-7983 919720.
- Naik, H., Prajapati, P.M., Suryanarayana, S.V., Jagadeesan, K.C., Thakare, S.V., Raj, D., Mulik, V.K., Shivashankar, B.S., Nayak, B.K., Sharma, S.C., Mukherjee, S., Sarbjit Singh, , Goswami, A., Ganesan, S., Manchanda, V.K., 2011. Measurement of the neutron capture cross-section of ^{232}Th using the neutron activation technique. *Eur. Phys. J. A* 47, 689–697.
- Nuttin, D., Heuer, D., Billebaud, A., Brissot, R., Brun, C.Le., Liatard, E., Loiseaux, J.M., Mathieu, L., Meplan, O., Merle-Lucotte, E., Nifenecker, H., Perdu, F., David, S., 2005. Potential of thorium molten salt reactors: detailed calculations and concept evolution with a view to large scale energy production. *Proc. Nucl. Energy* 46, 77–99.
- Paradela, C., et al., 2006. N-TOF fission data of interest to GEN-IV and ADS. In: Advances in Nucl. Analysis and Simul. (PHYSOR2006), Vancouver, Canada, pp. B076.
- Perkin, J.L., O’connor, L.P., Colemann, R.F., 1958. Radiative capture cross sections for 14.5 MeV neutrons. *Proc. Phys. Soc. (London)* 72, 505–513.
- Poenitz, W.P., Smith, D.L., 1978. Fast Neutron Radiative Capture Cross Section of ^{232}Th . Rept. Argonne National Laboratory Reports No. 42.
- Pomerance, H., 1952. Thermal neutron capture cross sections. *Phys. Rev.* 88, 412–413.
- Poppe, C.H., Anderson, J.D., Davis, J.C., Grimes, S.M., Wong, C., 1976. Cross section for the $^7\text{Li}(p, n)^7\text{Be}$ reaction between 4.2 and 26 MeV. *Phys. Rev. C* 14, 438–445.
- Pronyaev, V.G., 1999. Summary Report of the Consultants’ Meeting on Assessment of Nuclear Data Needs for Thorium and Other Advanced Cycles, INDC (NDS) – 408 (International Atomic Energy Agency).
- Raics, P., Daroczy, S., Csikai, J., Kornilov, N.V., Baryba, V.Ya., Salnikov, O.A., 1985. Measurement of the cross sections for the $^{232}\text{Th}(n, 2n)^{231}\text{Th}$ reaction in the 6.745 to 10.450 MeV energy range. *Phys. Rev. C* 32, 87–91.
- Rubbia, C., Rubio, J.A., Buono, S., Carminati, F., Fietier, N., Galvez, J., Geles, C., Kadi, Y., Klapisch, R., Mandrillon, P., Revol, J.P., Roche, Ch., 1995. Conceptual Design of a Fast Neutron Operated High Power Energy Amplifier, CERN/AT/95-44 (ET).
- Salvatores, M., 1997. Experimental facilities, training and expertise in the nuclear data field: Needs and gaps for reactor physics applications. In: Reffo, G., Ventura, A., Grandi, C. (Eds.), Proceedings of the International Conference on Nuclear Data for Science and Technology, Trieste, Italy, May 19–24, 1997, vol. 59. Part I, Italian physical Society, Bologna, pp. 3–17.
- Shibata, K. et al., 2011. JENDL-4.0: a new library for nuclear science and engineering. *J. Nucl. Sci. Technol.* 48, 1–30.
- Singh, B., Tuli, J.K., 2005. Nuclear data sheets for A = 233. *Nucl. Data Sheets* 105, 109–222.
- Sinha, R.K., Kakodkar, A., 2006. Design and development of the AHWR—the Indian thorium fuelled innovative nuclear reactor. *Nucl. Eng. Des.* 236, 683–700.
- Stupegia, D.C., Smith, B., Hamm, K., 1963. Fast neutron capture in ^{232}Th . *J. Inorg. Nucl. Chem.* 25, 627–630.
- The international Reactor Dosimetry File: IRDF-2002 (Nuclear Data Section, International Atomic Energy Agency, 2002).
- Westmeier, W., Brandt, R., Langrock, E.-J., Robotham, H., Siemon, K., Odoj, R., Adam, I., Bradnova, V., Golovatyuk, V.M., Krasnov, V.A., Krivopustov, M.I., Pronskikh, V.S., Sosnin, A.N., Tsoumpko-Sitnikov, V.M., Vladimirova, N.M., Hashemi-Nezhad, S.R., Zamani-Valasiadou, M., 2005. Transmutation experiments on ^{129}I , ^{139}La and ^{237}Np using the Nuclotron accelerator. *Radiochimica Acta* 93, 65–73.
- Wisshak, K., Voss, F., Kappeler, F., 2001. Neutron capture cross-section of ^{232}Th . *Nucl. Sci. Eng.* 137, 183–193.